

PYROLYSIS OF CHAR FORMING SOLID FUELS: A CRITICAL REVIEW OF THE MATHEMATICAL MODELLING TECHNIQUES

B. Moghtaderi

Department of Chemical Engineering, The University of Newcastle

AUSTRALIA

ABSTRACT

Recent advances in mathematical modelling and numerical analysis of the pyrolysis of char forming solid fuels have shed new light on the pyrolytic behaviour of these materials under fire conditions. A review of the pyrolysis models of charring solid fuels developed over the past 30 years is presented in the order of increasing complexity. The models can be broadly categorised into thermal and comprehensive type models. While thermal models predict the conversion of the virgin fuel into products based on a critical pyrolysis criterion and the energy balance, the comprehensive models describe the degradation of the fuel by a chemical kinetic scheme coupled with the conservation equations for the transport of heat and/or mass. A variety of kinetic schemes have been reported in the literature ranging from simple one-step global reactions to semi-global and multi-step reaction mechanisms. There has been much less uniformity in the description of the transport phenomena (i.e. heat and mass) in comprehensive models and different levels of approximation have been used. It is shown that the accuracy of pyrolysis models largely depends on the model parameters. If reliable data are not available, even the most advanced models give poor predictions.

Keywords: Pyrolysis, charring solid fuels, mathematical modelling, fires.

INTRODUCTION

Pyrolysis of solid fuels plays an important role in both the ignition and growth stages of fires. Whether a room fire will attain flashover depends on the total heat release rate associated with the combustion of the pyrolysis products. The pyrolysis phenomenon also plays a major role in the formation of smoke and toxic by-products.

In the context of fire safety, pyrolysis is almost exclusively referred to the thermal degradation of solid fuels due to external heating. Usually, the distinction is made between charring and non-charring fuels, based on the ability of the material to produce a char residue as it undergoes pyrolysis. Most cellulosic materials, such as wood, cardboard, paper, cotton, and certain thermosetting resins like Polyisocyanurate foam can be categorised as char forming solids. Other materials, such as Polymethylmethacrylate (PMMA), produce little or no char when they pyrolyse and, as such, they are referred to as non-charring materials.

Char forming (charring) solid fuels constitute a substantial fraction of the fuel load in many types of fires, particularly, building fires. For this reason an understanding of their behaviour under high temperature conditions is crucial. Generally, the pyrolysis of charring solid fuels is a complex phenomenon that involves a variety of physical and chemical processes, such as momentum, heat and mass transfer, property variations, structural changes, char oxidation and secondary chemical reactions within the solid (e.g. tar cracking). The pyrolysis process is also affected by factors such as oxygen concentration, irradiance, moisture content and the orientation of the solid fuel with respect to the external heat source (e.g. flames). A substantial amount of experimental and theoretical research has already been carried out on the pyrolysis of charring solid fuels under fire conditions. The primary objective of the experimental work, e.g.¹⁻⁶, has been the quantification of the chemical kinetics data (e.g. rates, regimes and mechanisms), heat of pyrolysis and mass loss rates.

The focus of modelling studies, however, has been on the analysis of the experimental data and in providing sub-models for room fire computer codes. There are a number of ways to classify the pyrolysis models of charring fuels. But perhaps the most logical approach is to categorise such models on the basis of the technique they use to describe the conversion of the virgin fuel into volatiles (i.e. gaseous products) and char residues. As such, the pyrolysis models can be classified into: (i) simple thermal models, and (ii) comprehensive models. The rate of fuel conversion (rate of pyrolysis) in thermal models is obtained from the energy balance while in comprehensive models a combination of kinetic schemes, mass and energy balance is employed to calculate the rate of pyrolysis. The thermal models, in turn, can be categorised into three main groups based on the solution approach. These are: (i) simple algebraic models, (ii) analytical models, and (iii) integral models. On the basis of solution approach, comprehensive models can be classified as: (i) analytical and (ii) numerical type models. However, it is perhaps more appropriate to classify comprehensive models according to the reaction schemes that they employ. Table A1 in Appendix A summarises the main features of a selected group of charring pyrolysis models.

The objective of this paper is to provide a critical review of the available modelling techniques for prediction of the pyrolytic behaviour of char forming solid fuels under fire conditions. The review is neither in chronological order nor an attempt to provide an exhaustive list of relevant publications. Instead, the review has been arranged according to nature of the pyrolysis models and a number of relevant key issues. Reference is frequently made to a selected group of well known models⁷⁻⁴⁰ (for a summary of the main features of these models see Table A1 of the Appendix A). It should be highlighted that there are a number of excellent reviews on pyrolysis modelling and simulation (for example the review paper by Di Blasi⁴¹). However, most of these surveys cover more than one type of solid fuels and none of the existing reviews include recent work of the last 8 years. Therefore, an up-to-date literature review of these new works appears to be in order.

SIMPLE THERMAL MODELS

In thermal models the chemical kinetics of the pyrolysis process is decoupled from other processes involved based on the assumption that pyrolysis occurs when the temperature reaches a so-called pyrolysis temperature. This assumption is not unrealistic because the activation energy for pyrolysis of most charring solids is generally quite high and, as such, the thermal decomposition process abruptly begins when the temperature reaches a critical level. The application of the critical pyrolysis temperature, however, greatly simplifies the problem and reduces the model into a purely thermal one where only an energy balance needs to be carried out. As pointed out earlier, in terms of the solution techniques, there are three different classes of thermal models. Algebraic and analytical models are briefly discussed in section 2.1 while a more detailed discussion about integral models is presented in section 2.2.

2.1 ALGEBRAIC AND ANALYTICAL MODELS

The idea behind algebraic and analytical thermal models is to obtain a closed form solution for the rate of fuel pyrolysis (i.e. mass loss rate) using the critical pyrolysis temperature criterion. To achieve this task, one needs to ignore most of the physical and chemical processes involved in order to reduce the complexity of the problem. In some cases, this may allow desired solutions to be obtained from an analytical analysis only. However, even analytical solutions are not often in suitable forms for any practical application (e.g. correlation of experimental data). Therefore, one needs to make further simplifications in the analytical solution to obtain the so-called algebraic solutions. To show the concept, the following cases will be examined.

Consider a thermally thin^a slab of fuel subjected to a constant heat flux. If it is assumed that the solid does not shrink or expand during pyrolysis, ignore the porous structure of the fuel and neglect variations in its thermophysical properties, then the energy conservation gives the rate of mass loss as²⁸:

$$\dot{m} = -\frac{\dot{q}_e'' A_s}{Q_p} \quad (1)$$

Equation 1 is obviously an easy to use analytical solution that can be conveniently employed in practical applications. Now, consider a thermally thick fuel sample subjected to a constant heat flux. Unlike, the previous case, the temperature will not be uniform within the solid. Thus, the transient heat conduction equation should be solved to obtain the temperature distribution within the solid. Pyrolysis can be assumed to occur at any location where the local temperature exceeds the critical pyrolysis temperature (T_p). Unfortunately, the analytical solution to the heat conduction equation under the specified conditions⁴² involves an infinite series and roots of the characteristic transcendental equation $\beta \cot(\beta) = 0$, which are difficult to use. However, a close examination of the first term in the infinite series solution reveals that this term remains roughly equal to 0.7 throughout the pyrolysis process. Using this value and neglecting other terms in the series, simplified algebraic expressions²⁸ can be derived for the temporal location of the pyrolysis front (x_p at which $T = T_p$) and the thermal wave speed (dx_p/dt). The mass loss rate can then be approximated by Equation 2. The system of equations for x_p , dx_p/dt , and \dot{m} , therefore, forms an algebraic thermal model.

^a Whether a sample of charring solid fuel is thermally thin or thick can be judged based on the Biot number which for a constant heat flux condition is defined as: $Bi = (\dot{q}_e'' \Delta x)/(k \Delta T)$. If $Bi \leq 1$ the solid fuel is regarded as thermally thin whereas it is thermally thick if $Bi \gg 1$.

$$\dot{m} = -A_s(\rho_0 - \rho_c) \left(\frac{dx_p}{dt} \right) \quad (2)$$

It should be highlighted that despite their simplicity and convenience, closed form solutions obtained from either exact (analytical models) or approximate (algebraic model) analysis have a limited range of applicability since a comprehensive solution that can be applied to any possible situation is generally not available.

2.2 Integral Models

Integral type thermal models employ numerical algorithms to obtain the temperature distribution and the mass loss rate in a pyrolysing charring fuel. Integral models are generally less restrictive than algebraic and analytical thermal models as they take into account many of the physical phenomena ignored in simple models. However, integral models like all other thermal models are based on the critical pyrolysis temperature criterion and, therefore, they neglect the role of the chemical kinetics in the overall thermal decomposition process. The biggest advantage of integral models is that they are relatively simple, easy to use, and computationally economic. This is because in integral models the partial differential equations governing the conservation of energy (i.e. heat conduction) are reduced to ordinary differential equations. This provides significant savings in CPU (central processing unit) time since the solution of an ordinary differential equation (ODE) is less time consuming than that of a PDE, but the results are obviously not as accurate as those of the original equations.

In integral models the original set of PDEs that describe the problem is reduced to a set of ODEs by assuming that the temperature distribution within the solid depends on the space variable (x) in some particular fashion consistent with the boundary conditions. The temperature distribution is then substituted into the heat conduction equation and integrated with respect to the space variable over appropriate intervals to obtain the so-called heat-balance integral. This results in a set of ordinary differential equations with time (t) as the independent variable. The success of the integral modelling depends crucially on the choice of the assumed temperature profile. A wide range of these profiles, including polynomial^{9,35,40} and exponential²⁵ temperature profiles, have been reported in the literature. However, it seems that a quadratic temperature profile is a reasonable choice because it is simple, satisfies typical boundary conditions and correlates the experimental data quite accurately^{35,40}. The remaining part of this section is devoted to the examination of an integral model based on such quadratic temperature profile³⁵.

The analysis begin with the physical description of this model and consider a slab of charring solid fuel exposed to an external heat source (e.g. a fire environment). The sequence of events occurring in the slab under specified conditions can be divided into three distinct phases⁹. These are: (i) the constant density heat-up phase, (ii) the infinite-body pyrolysis phase, and (iii) the finite-body pyrolysis phase. In the first phase the surface and interior temperatures of the slab rise with time as a thermal wave penetrates inside the material. The effect of the thermal

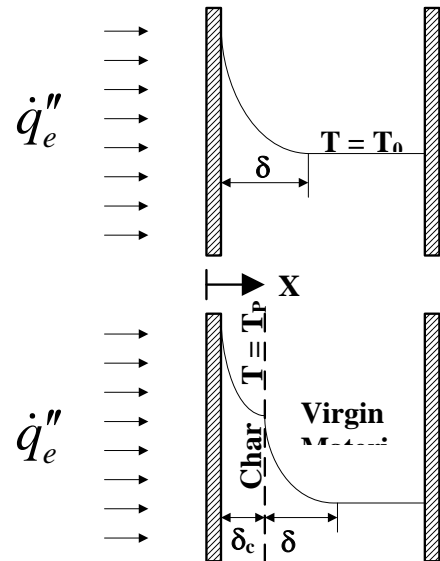


Figure 1: The physical configuration of the model.

wave is confined to a layer near the exposed surface (see Figure 1a) called the ‘thermal penetration depth (δ)’. As heating continues, the surface temperature increases until it satisfies the critical pyrolysis temperature criterion. This marks the start of the infinite-body pyrolysis phase in which the material behaves as a thermally thick solid. As Figure 1b illustrates, the initial depth can now be divided into two layers representing the char and virgin materials. Continuation of the pyrolysis process results in the growth of the char layer and deeper penetration of the thermal wave into the virgin layer. Once the thermal wave reaches the back face of the slab, the material begins to behave as a thermally thin solid marking the start of the finite-body pyrolysis phase. As a demonstration, the mathematical formulation of the infinite-body pyrolysis phase is derived in this section. More details, particularly about the heat-up and finite-body pyrolysis phases, can be found in Moghtaderi³⁵ et al..

Assuming that the heat transfer process is one-dimensional, thermophysical properties (e.g. thermal conductivity) are constant, the material does not contract or expand during pyrolysis, and the pyrolysis gases reach the exposed surface as soon as they formed at the pyrolysis front (δ_c). Assumptions of quadratic temperature profiles (Equations 3 and 4) for the temperature distributions in the char and virgin layers give rise to six new unknowns; $a_0(t)$, $a_1(t)$, $a_2(t)$, $b_0(t)$, $b_1(t)$, and $b_2(t)$. These unknowns together with δ_c and δ , as well as, two new variables defined by Equations 5 and 6 are all that are needed to calculate in order to fully solve the problem.

$$T_c(x,t) = a_0(t) + a_1(t)(\delta_c - x) + a_2(t)(\delta_c - x)^2 \quad (3)$$

$$T_v(x,t) = b_0(t) + b_1(t)(x - \delta_c) + b_2(t)(x - \delta_c)^2 \quad (4)$$

$$\theta_c = \int_0^{\delta_c} [T_c(x,t) - T_p] dx \quad (5)$$

$$\theta_v = \int_{\delta_c}^{\delta_c + \delta} [T_v(x,t) - T_p] dx \quad (6)$$

Ten equations are required to determine all unknowns. These can be derived from the heat conduction equations for char and virgin layers (Equations 7 and 8), initial conditions (Equations 9 and 10), boundary conditions (Equations 10-14), Stefan condition at the pyrolysis front (Equation 15), and finally the equation for volatile mass flux (Equation 16, mass loss rate per unit area).

$$\frac{\partial T_c(x,t)}{\partial t} = \alpha_c \frac{\partial^2 T_c(x,t)}{\partial x^2} \quad (7) \quad , \quad \frac{\partial T_v(x,t)}{\partial t} = \alpha_v \frac{\partial^2 T_v(x,t)}{\partial x^2} \quad (8)$$

$$T_c(0,t_p) = T_p \quad (9) \quad , \quad T_v(0,t_p) = T_p \quad (10)$$

$$-k_c \frac{\partial T_c(0,t)}{\partial x} = \dot{q}_{net} = \dot{q}_e'' - (\dot{q}_{l,rad}'' + \dot{q}_{l,conv}'') \quad (11) \quad , \quad k_v \frac{\partial T_v(\delta,t)}{\partial x} = 0 \quad (12)$$

$$T_c(\delta_c,t) = T_p \quad (13) \quad , \quad T_v(\delta,t) = T_0 \quad (14)$$

$$k_v \frac{\partial T_v(\delta_c,t)}{\partial x} - k_c \frac{\partial T_c(\delta_c,t)}{\partial x} = \dot{m}'' Q_p \quad (15) \quad , \quad \dot{m}'' = (\rho_v - \rho_c) \times \frac{d\delta_c}{dt} \quad (16)$$

To obtain the necessary equations one needs to: (i) substitute the quadratic temperature profiles (Equations 3 and 4) into Equations 7-16, (ii) integrate Equations 7 and 8 with respect to x over appropriate intervals^b, and (iii) carry out the necessary mathematical simplifications. This results in the following set of equations (Equations 17-26) that fully describes the problem.

$$\frac{d\delta_c}{dt} = \left(\frac{\alpha_v}{\alpha_v(\rho_v - \rho_c)Q_p - k_v(T_0 - T_p)} \right) \left(\dot{q}_{net}'' - \frac{k_c}{\alpha_c} \frac{d\theta_c}{dt} + \frac{k_v}{2\alpha_v} \frac{d\theta_v}{dt} \right) \quad (17)$$

^b From 0 to δ_c for the char layer and from δ_c to $\delta_c + \delta$, for the virgin layer.

$$\frac{d\theta_v}{dt} = \left(\frac{8\alpha_v(T_0 - T_p)^2}{3\theta_v} \right) - 2(T_0 - T_p) \frac{d\delta_c}{dt} \quad (18)$$

$$\frac{d\theta_c}{dt} = 3\alpha_c \left(\frac{\dot{q}_{net}''}{2k_c} - \frac{\theta_c}{\delta_c^2} \right) \quad (19), \quad \delta = \frac{3\theta_v}{2(T_0 - T_p)} \quad (20)$$

$$a_0(t) = T_p \quad (21), \quad a_1(t) = \frac{3\theta_c}{\delta_c^2} - \frac{\dot{q}_{net}''}{2k_c} \quad (22), \quad a_2(t) = \frac{-3\theta_c}{\delta_c^3} + \frac{3\dot{q}_{net}''}{4k_c\delta_c} \quad (23)$$

$$b_0(t) = T_p \quad (24), \quad b_1(t) = \frac{-2(T_p - T_0)}{\delta} \quad (25), \quad b_2(t) = \frac{(T_p - T_0)}{\delta^2} \quad (26)$$

The numerical solution of the above set of equations provides all the unknowns. The mass flux can be then calculated from Equation 16. The rate of pyrolysis (mass loss rate), in turn, is obtained from the product of \dot{m}'' and the surface area of the slab: $\dot{m} = \dot{m}'' \times A_s$.

3. Comprehensive models

From a mathematical point of view, the critical pyrolysis temperature criterion used in thermal models is equivalent of assuming that the chemical processes are much faster than diffusion processes. In other words, it is assumed that the entire pyrolysis process is diffusion controlled. In reality, the situation can be quite different. For instance, consider a 2cm-thick slab of wood having a volumetric thermal capacity (ρc) of 10^5 (J m⁻³ K⁻¹) and a thermal conductivity (k) of 10^{-1} (W m⁻¹ K⁻¹). The characteristic time for the pyrolysis process can be estimated from: $t_{ch} = 1/[A \exp(-E/RT)]$; and for the conduction heat transfer process from: $t_{ch} = (L^2 \rho c)/k$, where L is the slab thickness. For wood species the activation energy and pre-exponential factor of the pyrolysis process are typically in the order of 10^5 (J mol⁻¹ K⁻¹) and 10^8 (s⁻¹), respectively. As a result, the characteristic pyrolysis times at 470 K and 900 K are roughly 1.3×10^3 (s) and 6.4×10^{-3} (s), respectively. On the other hand, for the slab under consideration, the characteristic time of the heat conduction process is about 200 (s). Obviously, at high temperatures the conduction is several orders of magnitude slower than the chemical reaction rate and, hence, determines the pyrolysis rate. However, this is not the case for low temperatures (e.g. 470 K) as the conduction heat transfer is about 7 times faster than the chemical reaction rate. Therefore, the global pyrolysis at low temperatures is controlled by chemical kinetics whereas it is diffusion controlled at high temperatures. Since the transient pyrolysis of charring solids, particularly in building fires, occurs over a wide range of temperatures (typically between 450-1000 K), both diffusion and chemical kinetics should be taken into account. Comprehensive pyrolysis models have been developed based on this philosophy. In most cases chemical processes have been modelled based on first order kinetic schemes. These schemes range in complexity from one-step global^{10-12,14,17,19,20,30,39} to one-stage multi-reaction^{18,22,33,34,36} and two-stage semi-global^{16,21,23,26,27,29,31,37,38} schemes involving both primary and secondary reactions.

There has been much less uniformity in the description of the physical processes and different levels of approximation have been used in the modelling of these processes. The simplest approach consists of a heat conduction equation written for a constant property, non-porous solid¹⁷. The heat release due to chemical processes is included in the model via a source term. A more realistic approach was taken by Kung¹⁰ who added a number of new features to the simple approach, including variable thermo-physical properties and the convective heat transfer due to outward flow of volatiles. Kung's model was further developed by many other researchers to account for porous structure of the

solid^{11,21,23,26,27,29-31,36-39}, structural changes (e.g. swelling) during pyrolysis^{18,29} and the effect of fuel moisture content^{16,18,22,34,36}.

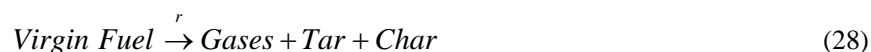
Comprehensive models are almost^c exclusively solved by numerical routines (Table A1), such as finite difference and finite volume methods. In these techniques the physical domain is discretised into cells of finite size. The collection of cells form a grid (mesh) which, depending on the solution strategy, can be one- two- or three-dimensional. The partial differential equations describing the problem are then discretised on the grid cells, resulting in a system of strongly coupled simultaneous algebraic equations. Because of the highly non-linear nature of these algebraic equations, all unknowns must be evaluated by iteration.

This section is concerned with examining the key features of comprehensive pyrolysis models, including: the kinetic schemes, transport phenomena, and the treatment of the fuel moisture content.

3.1 Kinetic Schemes

As pointed out earlier, kinetic schemes can be classified into three main groups⁴¹: (i) one-step global schemes, (ii) one-stage multi-reaction schemes, and (iii) two-stage semi-global schemes. A brief description of these schemes is presented in this section. For more details, the readers are referred to review papers by Di Blasi⁴¹; and Antal et al⁴⁵.

The one-step global schemes use a very simple mechanism to describe the conversion of the virgin fuel to products which can be either (a) volatiles and char, or (b) gaseous products, tar and char (Equations 27 and 28).



The rate of reaction (r) is expressed in an Arrhenius fashion (Equation 29) and considered to be proportional either to the weight residue or the weight loss of the fuel. The necessary kinetic parameters are generally obtained experimentally^{41,45} using thermogravimetric analysers (TGA), tube furnaces, fluidised bed reactors, and *in situ* measurement techniques.

$$r = A \exp(-E / RT) \quad (29)$$

The large diversity of charring solid fuels, particularly wood-based materials and biomass, has motivated analyses of somewhat less complex case of cellulose pyrolysis. In general, wood-based and biomass fuels are composed of approximately 50-60% cellulose by mass and, as such, many of kinetic characteristics of cellulose pyrolysis are common to all biomass and wood-based type fuels⁴⁵. Table 1 provides a summary of typical kinetic parameters for cellulose. The large differences in the estimated values of kinetic constants can be attributed to the different experimental conditions^d used by various researchers.

^c To the best of author's knowledge there is only one comprehensive model of analytical nature for charring pyrolysis in the open literature¹⁷. There are, however, a handful of papers dealing with analytical analysis of the pyrolytic behaviour of non-charring solids^{43,44}.

^d This changes the transport phenomena (heat, mass and momentum) leading to different pyrolytic behaviour.

Table 1: Typical kinetic data for one-step global pyrolysis of cellulose.

T (K)	E (kJ mol ⁻¹)	A (s ⁻¹)	Reference
600-850	100.5	1.2×10 ⁶	[45]
580-1070	8.8-33.4	0.019-0.14	[46]
450-700	71	6.79×10 ³	[47]
520-1270	139.6	6.79×10 ⁹	[47]
520-1270	166.4	3.9×10 ¹¹	[48]

The major limitation of one-step global schemes is that they are neither able to predict the composition of volatiles nor account for various components of the virgin fuel. These information, though, can be quite important in some applications. For example, in ignition related studies it is important to know the composition of volatiles because the heat content and flammability limits of the volatile mixture are determined by its composition. Similarly, for fuels like wood which compose of constituents (e.g. cellulose, hemicellulose, and lignin) with different chemical kinetic behaviour, it is often erroneous to lump all constituents together and treat the virgin fuel as a homogeneous solid. One-stage multi-reaction schemes have been developed to address these shortcomings. For cases concern with volatile composition it is often assumed that the virgin fuel decomposes directly to each product according to a series of parallel independent reactions of the form shown in Equation 30. For cases involving inhomogeneous fuels (e.g. biomass, wood, etc), one-stage reactions are written for each constituent (Equation 31). The overall rate of pyrolysis is then considered to be the sum of the rates of the individual constituents in a fashion consistent with their percentage in the virgin fuel. The scheme presented by Alves et al²² is an example of this type of multi-reaction schemes. These authors considered six independent first-order reactions for the pyrolysis of pine wood sawdust. Of these reactions, one corresponds to cellulose, one to hemicellulose, and four to lignin macromolecule.



The major shortcoming of the one-stage multi-reaction schemes is that they neglect secondary reactions (cracking of tar to light molecular weight volatiles). However, at high temperatures and sufficiently long residence times the extent of secondary reactions is significant and, thus, both primary and secondary reactions should be taken into account.

Two-stage semi-global schemes attempt to address this shortcoming of multi-reaction schemes by considering reaction routes for both primary and secondary reactions. Di Blasi⁴¹ and Antal et al⁴⁵ have compiled a comprehensive list of two-stage semi-global schemes in their review papers. Two of such kinetic schemes⁴¹ which have been widely used for cellulose and wood are presented in this section. Both schemes employ a simplified decomposition of the virgin fuel to form three lumped product groups, that is, char, heavy molecular weight tar vapours, and low molecular weight gases (Figure 2). All reactions are assumed to be first order, irreversible and follow Arrhenius law (Equation 29). Kinetic parameters for these two reaction schemes are given in Table 2.

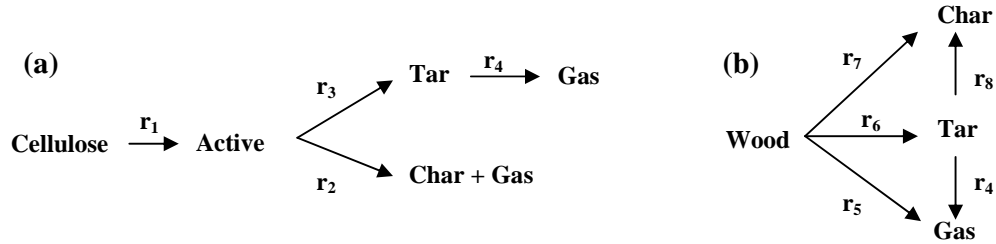


Figure 2: Two-stage semi-global reaction schemes for (a) cellulose and (b) wood.

Table 2: Kinetic data for two-stage semi-global pyrolysis of cellulose and wood⁴¹.

Cellulose			Wood		
Reaction	E (kJ/kmol)	A (s ⁻¹)	Reaction	E (kJ/kmol)	A (s ⁻¹)
1	2.424×10 ⁵	2.80×10 ¹⁹	4	1.080×10 ⁵	4.28×10 ⁶
2	1.505×10 ⁵	1.30×10 ¹⁰	5	8.86×10 ⁴	1.43×10 ⁴
3	1.965×10 ⁵	3.28×10 ¹⁴	6	1.127×10 ⁵	4.13×10 ⁶
4	1.080×10 ⁵	4.28×10 ⁶	7	1.065×10 ⁵	7.38×10 ⁵
			8	1.080×10 ⁵	1.00×10 ⁵

3.2 Transport Phenomena

The transient pyrolysis of charring solid fuels involves a series of complex phenomena, such as heat conduction, heat loss/gain due to chemical reactions, convective thermal transport due to the outward flow of volatiles, internal convective heat transfer between the volatiles and the solid matrix, accumulation of volatiles within the solid and subsequent pressure build-up within its porous structure, and desorption of fuel moisture content due to external heat. Obviously, it is not possible to provide a mathematical description of all processes involved as many of these processes are not well understood. Therefore, even a comprehensive mathematical model inevitably involves assumptions and approximations which should be based upon sound physico-chemical principles. Such assumptions can be made by evaluating the relative importance of each major phenomenon. To demonstrate this, an analysis similar to that of Chan et al¹⁶ is employed here in order to estimate the characteristics times of the main physical phenomena involved in the transient pyrolysis of wood. Due to the diversity of thermo-physical properties within and between wood species, typical values for Australian Radiata pine are used in this analysis.

Now consider a 2 cm thick slab of wood. If the sample is exposed to external heating on its top face, the length-scale of interest (L) will be the sample thickness. Using this length-scale,^e the characteristics times can be estimated of diffusion mass transfer, mass transfer by the flow of volatiles, internal

^e Note that the time-scales presented in Table 3 provide only an estimate of the real time and they do not reflect the magnitude of the driving force involved in each particular process.

convective heat transfer, and conduction heat transfer by Equations 32 to 35, respectively (Table 3). The results for temperatures of 500 K and 900 K are summarised in Table 3. The temperature and density dependencies of the thermo-physical properties (e.g. thermal conductivity) have been explicitly included using the relationships given in Wood Handbook⁵⁰. The values of typical properties at 500 K are given in Table 4.

Table 3: Characteristics time-scales of the major physical processes in the pyrolysis of wood.

Phenomenon	Equation	Characteristic Time-Scale (s)	
		At T = 500 K	At T = 900 K
Diffusion mass transfer	$t_{ch} = L^2/D_{eff}$ (32)	400	120
Mass transfer by volatile flow	$t_{ch} = \mu L^2/PK_0$ (33)	13	10
Internal convective heat transfer	$t_{ch} = Ld(\rho c)/h$ (34)	0.1	0.1
Conduction heat transfer	$t_{ch} = L^2(\rho c)/k$ (35)	200	> 200

Table 4: Typical thermo-physical properties of wood at 500 K.

Symbol	Description	Value
D_{eff}	Effective mass diffusivity	10^{-6} (m ² s ⁻¹)
μ	Viscosity	10^{-5} (Pa s)
P	Volatiles over pressure	300 (kPa)
K_0	Permeability in the longitudinal direction	10^{-14} (m ²)
ρc	Volumetric thermal capacity of the solid	10^5 (J m ⁻³ K ⁻¹)
k	Thermal conductivity	10^{-1} (W m ⁻¹ K ⁻¹)
h	Internal heat transfer coefficient	10 (W m ⁻² K ⁻¹)
d	The characteristic diameter of a typical pore (10 μ m) divided by L	5×10^{-4}

As can be seen in Table 3, at all temperatures, the mass transfer by diffusion is far slower than the mass transfer by the hydrodynamic flow of volatiles (i.e. convective mass transfer). As a result, the volatile release can be regarded as an instantaneous process. Therefore, the accumulation of mass and energy of gaseous products within the solid matrix should be negligible. In other words, the transport phenomena of the gas-phase (volatiles) can be assumed to be a quasi-state process. If the pressure variation inside the porous solid is also neglected, the solid can be treated as a non-porous (i.e.

homogeneous) media. This assumption has been employed in many comprehensive pyrolysis models, particularly in the earlier models^{10,12,14,16,18,22,33-34}.

There are, however, many situations where the assumption of non-porous structure for the solid is not justified. For instance, some researchers^{51,52} have found that for woods of similar densities but widely varying longitudinal permeabilities subjected to similar heat flux levels, the rate of pyrolysis (i.e. fuel conversion) varies considerably. They have argued that the pressure build-up within the porous structure of the fuel may have a marked effect on its permeability which, in turn, may affect the course of the pyrolysis process. For this reason, a number of researchers have treated the charring solid fuels as porous mediums and taken into account the pressure variation inside the porous solid using the Darcy law^{11,23,27,29-31,36-39}. There are also models²¹ where the non-isobaric mass transport through the porous medium is accounted for using the 'dusty gas' flux equations (for details⁴¹).

The internal convective heat transfer between the volatiles and solid matrix is also one of the major physical processes involved in the transient pyrolysis of charring fuels. However, as Table 3 shows, for the Radiata pine specimen under consideration a rather short characteristic time is estimated for internal convection to occur. This short time-scale and the fact that the thermal capacity of the solid is much higher than the thermal capacity of volatiles (by at least two orders of magnitude) indicate that the solid matrix and volatiles must be in local thermal equilibrium state, that is $T_{solid} = T_{gas}$. Therefore, it is reasonable to ignore the details of internal convection and to assume thermodynamic equilibrium^{10,34}.

To examine the relative importance of the convective heat transfer due to the outward flow of volatiles, the following Peclet number can be used which is similar to that proposed by Kanury⁵³ in 1970:

$$Pe \equiv \frac{\text{Convective Transport of Energy by Volatile Outflow}}{\text{Heat Transfer by Conduction}} \equiv \frac{c_g \dot{m}'' L}{k} \quad (34)$$

where c_g and \dot{m}'' represent the specific heat and the total mass flux of volatiles, respectively. If $Pe \ll 1$, then convection effects will be small compared with the effects of conduction and, hence, the convective thermal transport of volatiles can be ignored. If, however, $Pe > 1$ the convection is not negligible and should be taken into account.

For the present analysis \dot{m}'' can be approximated at 50 (g m⁻² s⁻¹) based on the data extracted from experiments conducted in a cone calorimeter at heat flux levels between 25-65 kW/m². Using this value for volatile mass flux in conjunction with values of 0.1 (W m⁻¹ K⁻¹) and 1.03 (kJ kg⁻¹ K⁻¹) for the thermal conductivity of wood and the specific heat of volatiles, respectively, one obtains a value of 10.3 for the Peclet number from Equation 34. Similar analysis carried out by the author³⁴ for wood species other than Radiata pine revealed that the values of Peclet number were always much greater than unity. Therefore, it appears that neglecting the convective thermal transport of volatiles could create large errors in the final results and, hence, it should be taken into account.

3.3 Treatment of the Fuel Moisture Content

Among charring solid fuels wood-based materials naturally contain some moisture which exists in two basic forms: (i) bound or hygroscopic water, and (ii) free or capillary water⁵⁴. Bound water that is found in the cell wall is bonded to the hydroxyl groups of the major constituents of wood including cellulose, hemicellulose, and lignin. The free water, however, is present in the liquid form in the lumens or voids of the wood. There is no hydrogen bonding and, as such, free water is held only by

weak capillary forces. When only bound water is present an equilibrium exists between the relative humidity of the surrounding air and the moisture content of the wood. The cell walls become saturated as the relative humidity of the ambient approaches 100%. Beyond this point, which is called *Fibre Saturation Point* (FSP), additional water exists only in the form of free water. For most wood species the moisture content at FSP is about 30% while the total moisture content could be as high as 60%. This indicates that under normal conditions both free and bound water exist in wood highlighting the large amount of water that can be absorbed.

When moist wood is subjected to external heating, it first undergoes an initial drying period that begins when the exposed surface reaches a temperature near 100°C. During this initial period, most of the energy received by the fuel is consumed by heating and evaporating of the free water portion of the total moisture content. As drying proceeds, the total moisture content of the surface drops to levels close to FSP and, as a result, an evaporation front begins to travel into the solid, leaving behind a zone with a moisture content below the FSP. While ahead of the evaporation front the moisture is still in the form of liquid water, behind the front moisture exists only in the form of water vapour. The main mass transfer processes occurring behind the evaporation front are the convective and diffusive transport of water vapour, as well as, the diffusion of the bound water across the cell walls. When the material undergoes pyrolysis at higher temperatures, the water vapour mixes with the volatiles formed from pyrolysis and flows out of the solid. This, in turn, impacts on the other heat and mass transfer processes taking place within the solid, ultimately affecting the progress of the pyrolysis process. Therefore, the fuel moisture content may significantly alter the pyrolytic behaviour of the fuel.

Despite its importance, the modelling of the moisture desorption has received far less attention than other phenomena involved in the pyrolysis of charring solid fuels. In fact, there are only a handful of models reported in the literature which consider the effect of moisture desorption on the pyrolysis process^{16,18,22,32,34,36,55}. For obvious reasons, most of such models are applicable to wood-based materials only. There are basically three different approaches to moisture desorption modelling. In these approaches the evaporation process is described: (i) as an additional chemical reaction^{16,18,32}, (ii) using a boiling temperature criterion^{22,32,34}, (iii) using local moisture-vapour equilibrium relations^{36,55}. The major short coming of models categorised in groups (i) and (ii) is that they ignore free water and, hence, are applicable to fuel samples with moisture contents below the FSP having similar longitudinal and transversal dimensions. Such restrictive assumptions are removed in moisture-vapour equilibrium type desorption models (see section 3.4).

3.4 A Comprehensive Pyrolysis Model

Based on the information presented in sections 3.2 and 3.3, a one-dimensional pyrolysis model, applicable to infinite slabs, infinite cylinders and spheres, can be formulated³⁶. The following assumptions are made in the derivation of the model:

- The material is assumed to have a porous structure. However, all structural changes (eg swelling, shrinkage, formation of cracks) during drying and pyrolysis are ignored.
- Heat conduction is calculated by allowing for variable thermo-physical properties. The thermal conductivity (k_s) and the specific heat (c_s) of the virgin material are assumed to be linear functions of the local temperature. The thermo-physical properties of the solid matrix are obtained by linear interpolation between the property values of the virgin fuel and char.
- Fuel is assumed to consist of a series of different chemical components. For each component pyrolysis follows a one-step (global), first-order Arrhenius reaction scheme.

- The contribution of the thermal decomposition to the local energy balance is expressed as a volumetric heat source. The heat of pyrolysis associated with this source term is assumed to be constant.
- It is assumed that local thermal equilibrium exists between the fluid and solid, hence, a model for internal convection is not required.
- Liquid-vapour equilibrium is assumed to exist in the presence of free water. As a result the partial pressure of the vapour is equal to the saturation pressure.
- Movement of both liquid and gases are taken into account using Darcy's law with variable coefficients.
- All species of interest are assumed to be far from their critical points and volatile materials as well as water vapour are treated as ideal gases.

The model is described by a number of governing equations including, energy, continuity (for gaseous and liquid species), Darcy's law and equations of state. The conservation of energy in a general coordinate system is expressed as:

$$\frac{\partial}{\partial t}(\rho c T) = \frac{1}{\lambda} \frac{\partial}{\partial x} \left(\lambda k \frac{\partial T}{\partial x} \right) + \frac{1}{\lambda} \frac{\partial}{\partial x} \left(\lambda \left(\rho_l c_l u_l + \rho_{mix} c_{mix} u_{mix} + \rho_{mix} D (c_g - c_v) \frac{\partial M_g}{\partial x} \right) T \right) - \left(\sum_i h_{pi} r_{ci} + H_{ev} r_{ev} \right) \quad (35)$$

where k , ρ and c are overall values which are obtained from the following relationships:

$$\rho c = \rho_s (1 - \varepsilon) c_s + \rho_{mix} \varepsilon \left(1 - \frac{\varepsilon_l}{\varepsilon} \right) c_{mix} + \rho_l \varepsilon c_l \quad (36)$$

$$k = \eta k_w + (1 - \eta) k_c + \varepsilon k_{mix} + \sigma T^3 d / \omega \quad (37)$$

$$\eta = \frac{\rho_s - \rho_c}{\rho_{s_0} - \rho_c} \quad (38)$$

$$\varepsilon_l = \rho_l / \rho_l^* \quad (39)$$

The initial and boundary conditions for the energy equation are:

$$T(x, 0) = T_0(x) \quad (40)$$

$$\frac{\partial T}{\partial x}(L, t) = 0 \quad (41)$$

$$-k \frac{\partial T}{\partial x} = \dot{q}_e'' - h(T - T_\infty) - \sigma \omega (T^4 - T_\infty^4) \quad (42)$$

The conservation of mass for volatile materials is given by Equation 43 with initial and boundary conditions (44) to (46). The corresponding equation for water-vapour is omitted as only one species equation is needed due to the fact that the overall gas-phase continuity is considered here.

$$\frac{\partial M_g}{\partial t} = D \frac{\partial^2 M_g}{\partial x^2} + \left(\frac{1}{\lambda \rho_{mix}} \frac{\partial}{\partial x} (\lambda \rho_{mix} D) + u_{mix} \right) \frac{\partial M_g}{\partial x} - \left(\frac{M_g \sum_i r_{ci}}{\rho_{mix}} \right) \quad (43)$$

$$M_g(x,0) = M_{g,0}(x) \quad (44)$$

$$\frac{\partial M_g}{\partial x}(L,t) = 0 \quad (45)$$

$$\rho_{mix} D \frac{\partial M_g}{\partial x}(0,t) = -h_D (M_g(0,t) - M_{g,\infty}(t)) \quad (46)$$

The velocity of the gas-phase (the mixture of volatile and water-vapour) is obtained from Darcy's law (Equation 47) with the boundary condition (48):

$$u_{mix} = -k_D \frac{\partial P}{\partial x} \quad (47)$$

$$P(0,t) = P_\infty \quad (48)$$

The conservation of mass for the gas-phase gives (Equation 49 with Equation 50 as boundary condition):

$$\frac{\partial \rho_{mix}}{\partial t} + \frac{1}{\lambda} \frac{\partial}{\partial x} (\lambda \rho_{mix} u_{mix}) = \sum_i r_{ci} + r_{ev} \quad (49)$$

$$u_{mix}(L,t) = 0 \quad (50)$$

The continuity equation for liquid is given by Equation 51 with the initial condition (52):

$$\frac{\partial \rho_l}{\partial t} = r_{l,in} - r_{ev} \quad (51)$$

$$\rho_l(x,0) = \rho_{l,0}(x) \quad (52)$$

Equations of state for the water-vapour and the gas-phase mixture are:

$$P_v \left(\varepsilon - \frac{\rho_l}{\rho_l^*} \right) = (1 - M_g) \rho_{mix} R_v T \quad (53)$$

$$P \left(\varepsilon - \frac{\rho_l}{\rho_l^*} \right) = \rho_{mix} R_{mix} T \quad (54)$$

Since liquid and vapour are assumed to be in equilibrium, $P_v = P_{sat}(T)$ in the presence of liquid water. A simple analytical expression reported by Sahota⁵⁶ is used to relate the saturation pressure to the temperature. This expression has the following form:

$$P_{sat}(T) = CT^{-B/R_v} \exp\left(\frac{-A}{R_v T}\right) \quad (55)$$

where $A = 3.18 \times 10^3$ (kJ kg⁻¹), $B = 2.5$ (kJ kg⁻¹ K⁻¹) and $C = 6.05 \times 10^{26}$ (N m⁻²). For component i the rate of pyrolysis is determined using a first-order Arrhenius reaction:

$$\frac{\partial \rho_i}{\partial t} \equiv r_{ci} = -\rho_i a_i \exp\left(\frac{-E_i}{RT}\right) \quad (56)$$

The set of Equations 35-56 describes the heat and mass transfer processes for the problem under investigation. For convenience, these equations are further recast in terms of the pressure. The unknowns are: temperature, volatile mass fraction, pressure, mixture mass average velocity, liquid density, production rates, gas-phase density and vapour partial pressure. It should be noted that the above system of equations can be applied to infinite slabs, infinite cylinders and spheres if they are transformed into

suitable forms. This can be done by setting $\lambda = 1$, $\lambda = x$ and $\lambda = x^2$ for infinite slabs, infinite cylinders and spheres, respectively.

4. Influence of the model type and assumptions on predictions

4.1 Integral Models Versus Comprehensive Models

In order to evaluate the predictive capabilities of the integral and PDE type comprehensive models, a number of comparisons are made in this section using the results reported in the open literature.

The first case deals with the heat-up (i.e. the phase prior to pyrolysis) of a thermally thick homogeneous slab of fuel exposed to a constant external heat flux. For this case, an exact analytical solution to the one-dimensional heat conduction equation can be obtained if re-radiation and convective heat losses are ignored. The result for the surface temperature of the solid is⁴²:

$$T_s - T_0 = \left(\frac{4\alpha t}{\pi} \right)^{0.5} \frac{\dot{q}_e''}{k} \quad (57)$$

For the same conditions it has been shown^{33,35} that there is a closed form solution to the integral model presented in section 2.2:

$$T_s - T_0 = \left(\frac{3\alpha t}{2} \right)^{0.5} \frac{\dot{q}_e''}{k} \quad (58)$$

By comparing Equations 57 and 58 it is seen that the results are of the same form, differing only by a numerical factor. Since $(4/\pi)^{0.5} = 1.13$ and $(3/2)^{0.5}$ is approximately 1.2, the difference is only about 6%. This difference, as shown in earlier work⁵⁷, can be reduced to about 1.4% if the heat-up sub-model is derived using the first two moments of the heat conduction equation. However, the model resulting from this approach is more computationally expensive than the present model because an additional differential equation has to be solved for the surface temperature.

The second case deals with a situation similar to the previous case except heat losses are taken into account here. The results for the measured and predicted surface temperatures corresponding to an external radiant heat flux of 20 kW/m² are summarised in Figure 3. The symbols represent experimental data acquired from tests conducted on oven-dry Radiata pine specimens in a cone calorimeter³⁴. Predictions were obtained from the comprehensive and integral models presented in sections 2.2 and 3.4, respectively. All material properties were obtained from data and empirical relations reported in the literature^{50,545}. As Figure 3 indicates, the integral model produces results which are in good agreement with those obtained from experiments. The integral model predictions are also very close to those of the comprehensive PDE model with a difference of about 2%. It has been reported in the literature⁵⁰ that integral models can also perform well under extreme conditions,

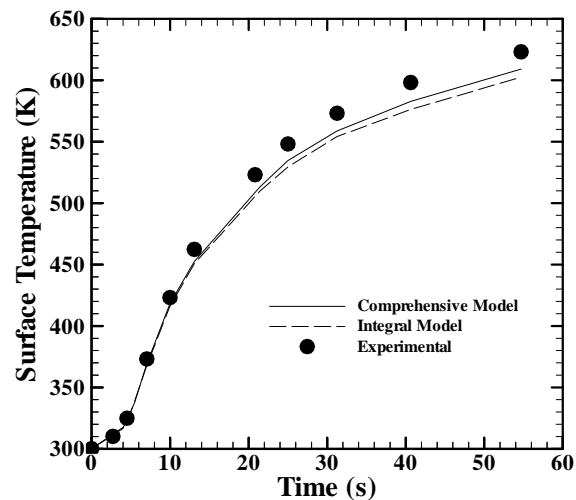


Figure 3: A comparison of the measured and calculated surface temperature for Radiata pine at a heat flux level of 20 kW/m².

such as a sudden step in the external heat flux and a variable external heat flux. However, they do not predict any physically meaningful results for situations where there is a cooling phase after a primary heating period. This is not surprising since under such conditions there is no longer a monotonic variation of the temperature with depth and, thus, the typical temperature profiles often employed in integral models are not valid.

The third case examines the accuracy of the integral and comprehensive models in predicting the main pyrolytic characteristics of charring solid fuels. This case shows a set of calculations in which the integral model predictions were compared with experimental data for pacific maple, as well as the numerical results from two comprehensive pyrolysis models. Comprehensive model (I) has a one-dimensional formulation, ignores the porous structure of the fuel, and treats the chemical kinetic using a single-step global reaction scheme. The readers are referred to Novozhilov³³ for more details about the kinetic parameters and thermo-physical properties used in this model. The same set of properties were used in the comprehensive model (II) which is basically the model described in section 3.4. The kinetic parameters needed for model (II) were obtained from the literature^{36,45}.

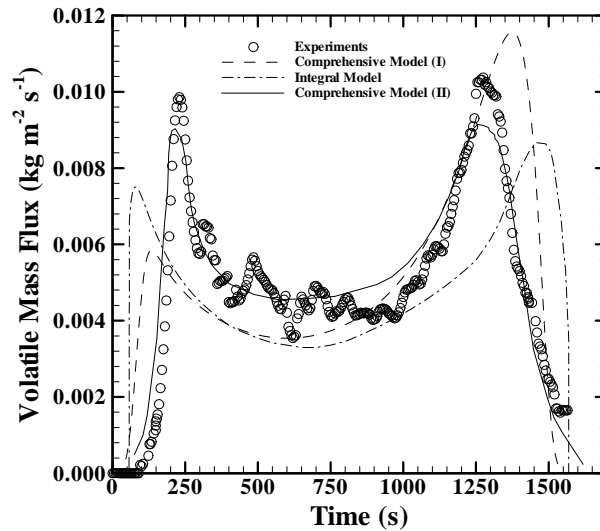


Figure 4: The predicted and measured mass loss rates for Pacific maple at a heat flux level of 20 kW/m².

Both comprehensive models and the integral model were incorporated as sub-models into a CFD code to simulate the combustion of Pacific maple samples in a standard cone calorimeter. Figure 4 indicates that despite the neglect of detailed chemical pyrolysis expressions, the integral model simulates the experimental data reasonably well with a maximum difference of 20% in the regions of the maximum volatile mass flux. The integral model, however, does not accurately predict the onset of pyrolysis mainly because the initiation of the pyrolysis process which occurs at relatively low temperatures is controlled by chemical kinetics rather than thermal transport (see section 3.2).

Similarly, the comprehensive model (I) provides a poor prediction of the onset of pyrolysis primarily because it employs a very simplified kinetic scheme. On the contrary, model (II) with its more sophisticated kinetic scheme, correctly predicts the start of the pyrolysis process and provides an accurate estimate of the first peak in the mass flux curve. In addition, since model (II) treats the solid as a porous media, it produces better predictions than the other models in the later stages of the pyrolysis process where transport processes are dominant.

For this particular case a sensitivity analysis was also carried out to evaluate the numerical performance of all models. It was found that for the same level of accuracy the integral model needed 47% and 52% less computing time than models (I) and (II), respectively. This can be assigned to the fact that the integral model solves only a set of ordinary differential equations that are computationally less expensive.

4.2 Influence of the Model Assumptions on the Performance of Comprehensive Models

The objective of this section is to illustrate the impact that model assumptions may have on the predictions of comprehensive pyrolysis models. For this purpose two cases are examined of which the first case deals with the transport phenomena while the second case emphasises on the moisture desorption modelling.

The first case is based on one of Di Blasi's⁵⁸ works in which models of different complexity were compared in order to understand the role played by model assumptions on the pyrolysis of cellulose in the heat transfer controlled regime. The reference model used by Di Blasi⁵⁸ was one-dimensional and included a full description of: (a) heat transport processes (i.e. conduction, convection, in-depth radiation), (b) unsteady gas-phase processes, (c) transport of volatile species (gas and tar) by convection and diffusion, (d) variable thermo-physical properties, and (e) porous media treatment of the solid. Four simplified versions of the reference model were examined of which only three are discussed here. These are: (i) constant property model, (ii) quasi-steady model, and (iii) constant pressure model. In the constant property model, the variation of thermo-physical properties with temperature and fuel conversion were simply ignored. In the second model the gas-phase processes were assumed to be quasi-steady, that is: negligible accumulation of mass and energy of volatiles within the solid. In the third model the porous structure of the solid was ignored by using the quasi-steady and no pressure gradient assumptions.

The effects of model assumptions on the yield of gaseous products as a function of the reactor temperature when 90% of the solid has been decomposed are shown in Figure 5. These results are related to a dry cellulose particle with a diameter of 5cm. As can be observed, there is a general qualitative agreement between the predictions of the reference model and those of the constant pressure and constant property models. While at high reactor temperatures differences become more pronounced, at lower temperatures the agreement is remarkably good. This is primarily due to the fact that at low temperatures neither the gas release rates are high to cause significant pressure variations, nor the spatial gradients of the local temperature are sufficiently large to generate noticeable changes in properties such as thermal conductivity. The predictions of the quasi-steady model are quantitatively and qualitatively different from those of the reference model. It is well known that quasi-steady models have a satisfactory performance for chemically controlled processes⁵⁸. However, for thermally controlled processes the predictions of quasi-steady models depend on the particle size and its physical properties (i.e. characteristic times for convective and diffusive mass transport, see section 3.2). For the case under investigation the particle length scale is relatively large and as a result the transport of mass by convection and diffusion should have similar characteristics times. Therefore, the quasi-steady model appears to be unsuitable for this case.

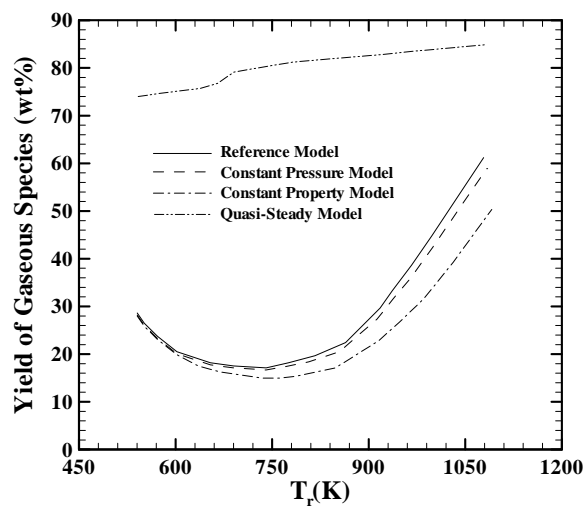


Figure 5: Gaseous product yield, in wt% of cellulose, for a 90% conversion of the virgin solid.

The second case deals with a comparison between Alves's²² experimental data and three different moisture desorption sub-models, incorporated in to a comprehensive pyrolysis model similar to that outlined in section 3.4. The experiments were carried out inside a vertical cylindrical refractory steel reactor surrounded by a furnace. The samples used were oven-dry and wet cylinders of pine. The length of the specimens was at least 3 times greater than their diameters. As a result, the data were considered representative of the pyrolysis of infinite cylinders. Six major components of wood were identified and their corresponding chemical kinetics data were measured experimentally. The thermo-physical properties of the virgin wood and char were also measured in the temperature range of 30-220 °C. Values of these thermo-physical and chemical properties are given elsewhere³⁶ and are not repeated here.

Figure 6 illustrate the comparison between the experimental thermograms and model predictions. Set (a) represents a sample with 18.2 mm diameter and 45% moisture content exposed to a reactor temperature of 780⁰C whereas set (b) represents a sample with 18.6 mm diameter and 46.3% moisture content exposed to a reactor temperature of 398⁰C.

As Figure 6 illustrates, under high temperature conditions where moisture desorption rate is relatively high, all models provide similar predictions. For low temperatures, however, the chemical reaction type model generates very poor predictions because of the neglect of the free water movement and moisture-vapour equilibrium. Both boiling temperature and equilibrium models correctly predict the trend of the experimental thermogram throughout the drying process. This can be mainly assigned to the fact that both of these models take into account the local equilibrium which exists between the vapour and moisture under low temperature conditions (i.e. low heating rates leading to slow moisture desorption rates). The predictions of the equilibrium model, however, are more accurate as it also takes into account the free water movement ignored by the boiling temperature model.

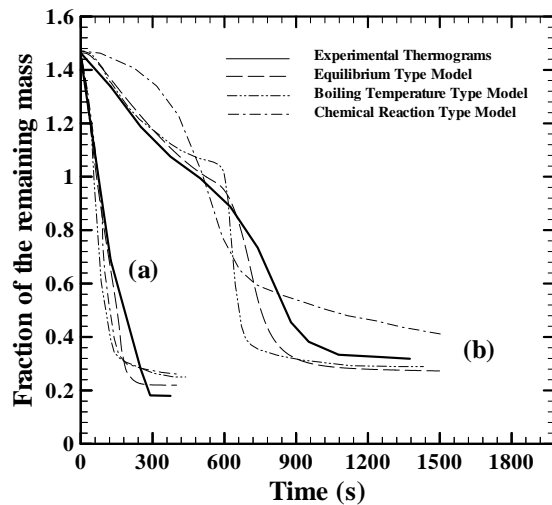


Figure 6: A comparison between the experimental and simulated thermogravimetric curves of wet wood cylinders.

5. CONCLUSIONS AND FUTURE WORK

Pyrolysis of charring solid fuels is the result of complex interactions among many physical and chemical processes. Mathematical modelling can be a very useful tool in examining the role played by these complex physical/chemical processes. A variety of mathematical modelling techniques available for analysis of charring pyrolysis were discussed in this paper. It was shown that the needs for proper description of major physical/chemical processes and acquisition of reliable property data often lead to complicated mathematical models. Numerical solution of such complex models, especially for two- or three-dimensional cases, is often time consuming and, therefore, computationally expensive. To overcome this problem simplifying assumptions for the description of the transport phenomena and

chemical processes can be introduced. The present paper aimed at providing an insight into when and how such simplifications can be made.

In the light of extraordinarily rapid progress in developing high powered ultra fast computing platforms, comprehensive pyrolysis models will become more affordable and, hence, will be the most logical forms of modelling techniques in the long run (next 10 years). For this reason research efforts should focus on further development of these comprehensive models. A especial attention must be given to the development of more accurate, general, and robust chemical kinetic mechanisms.

In the mean time both thermal models and the existing comprehensive models should be exploited more effectively. One suggestion is to use hybrid models in which a comprehensive type sub-model is used to carryout calculations related to the chemically controlled phase of the pyrolysis process while a thermal type sub-model is employed in the thermally controlled phase. Such hybrid models are currently being developed at the University of Newcastle.

NOMENCLATURE

A	Activation energy in Equation 55 [$\text{kJ mol}^{-1} \text{K}^{-1}$], Surface area (m^2)
a	Pre-exponential factor [s^{-1}]
a_0, a_1, a_2	Coefficients of the char layer quadratic temperature profile
B	Constant in Equation 55
b_0, b_1, b_2	Coefficients of the virgin layer quadratic temperature profile
C	Pre-exponential factor in Equation 55
c	Specific heat [$\text{kJ kg}^{-1} \text{K}^{-1}$]
D	Diffusion coefficient for Fick's law [$\text{m}^2 \text{s}^{-1}$]
d	Pore diameter [m]
E	Activation energy [$\text{kJ mol}^{-1} \text{K}^{-1}$]
H_{ev}	Latent heat of evaporation [kJ kg^{-1}]
h	Convective heat transfer coefficient [$\text{W m}^{-2} \text{K}^{-1}$]
h_D	Mass transfer coefficient [$\text{kg m}^{-2} \text{s}^{-1}$]
h_{pi}	Heat of pyrolysis of component i [kJ kg^{-1}]
K_0	Permeability [m^2]
k	Thermal conductivity [$\text{W m}^{-1} \text{K}^{-1}$]

k_D	Darcy's coefficient [$\text{m}^3 \text{s kg}^{-1}$]
L	Thickness [m]
M_g	Mass fraction of volatile materials in the gas phase
\dot{m}'	Mass loss rate [kg s^{-1}]
\dot{m}''	Mass flux [$\text{kg m}^{-2} \text{s}^{-1}$]
P	Pressure [Pa]
Q_p	Heat of pyrolysis [kJ m^{-3}]
\dot{q}''	Heat flux [kW m^{-2}]
R	Gas constant [8.314 J mol^{-1}]
r	Reaction rate [$\text{kg m}^{-3} \text{s}^{-1}$]
T	Temperature [K]
t	Time [s]
u	Velocity [m s^{-1}]
x	Space coordinate

Greek symbols

α	Thermal diffusivity [$\text{m}^2 \text{s}^{-1}$]
δ	Thermal penetration depth [m]
ε	Porosity
η	Progress variable in Equation 38
θ	Integral of the temperature profile (Equations 5 and 6)
λ	Geometric factor
μ	Viscosity [Pa s]
ρ	Density [kg m^{-3}]
ρ_l^*	Mass of liquid water per unit volume [kg m^{-3}]
σ	Stefan-Boltzman constant [$5.67 \times 10^{-8} \text{ W m}^{-2} \text{ K}^{-4}$]
ω	Emissivity

Subscripts

∞	Ambient
0	Initial condition
<i>c</i>	Char
<i>ch</i>	Characteristic
<i>ci</i>	Chemical reaction for <i>i</i> th component
<i>e</i>	External
<i>eff</i>	Effective
<i>ev</i>	Evaporation of water
<i>g</i>	Volatile materials
<i>i</i>	<i>i</i> th component
<i>l</i>	Liquid
<i>l, conv</i>	Heat loss due to convection
<i>l, rad</i>	Heat loss due to radiation
<i>mix</i>	Gas-phase mixture
<i>net</i>	Net value
<i>p</i>	Pyrolysis
<i>r</i>	Reactor
<i>s</i>	Solid material, Surface
<i>sat</i>	Saturation condition
<i>v</i>	Water-vapour, Virgin layer
<i>w</i>	Wood or virgin fuel

REFERENCES

- 1 Roberts, A.F., and Clough, G., *9th Symp. (Int.) on Combustion*, 158-166, 1963.
- 2 Kanury, A.M., and Blackshear, P.L., *11th Symp. (Int.) on Combustion*, 517-523, 1967.
- 3 Tewarson, A., and Pion, R., *Combustion and Flame*, 26, 85-103, 1976.
- 4 Vovelle, C., Akrich, R., and Delfau, J.L., *Combust. Sci & Technology*, 36, 1-18, 1984.
- 5 Vovelle, C., Akrich, R., and Delfau, J.L., *20th Symp. (Int.) on Combustion*, 1647-1654, 1984.
- 6 Shafizadeh, F., "The Chemistry of Pyrolysis and Combustion", In: *The Chemistry of Solid Wood*, Edited by Rowell R, American Chemical Society, 489-529, 1984.
- 7 Bamford, C., Crank, J., and Malan, D., *Proceedings of the Cambridge Philosophical Society*, 42, 162-182, 1945.
- 8 Kanury, A.M., *Fire Research Abstracts and Reviews*, 14, 24-52, 1971.
- 9 Kanury, A.M., *Combust. Sci & Technology*, 5, 135-146, 1972.
- 10 Kung, H.C., *Combustion and Flames*, 18, 185-195, 1972.
- 11 Kansa, E., Perlee, H., and Chaiken, R., *Combustion and Flames*, 29, 311-324, 1977.
- 12 White, R.H., Schaffer, E.L., *Fire Technology*, 14(4), 279-290, 1978.
- 13 Tewarson, A., Lee, J., and Pion, R., *FMRC Serial No J.I.OC6N2.RC*, USA, 1979.
- 14 Atreya, A., PhD Thesis, Harvard University, USA, 1983.
- 15 Delichatsios, M.A., and De Ris, J., *FMRC Serial No J.I.OKOJ1.BU*, USA, 1983.
- 16 Chan, W., Kelborn, M., and Krieger, B., *Fuel*, 64, 1505-1513, 1985.
- 17 Miller, C.A., and Ramohalli, K.N.R., *Combust. Sci & Technology*, 46, 249-265, 1986.
- 18 Parker, W.J., *Fire Safety Science-Proceedings of the 1st International Symposium*, 207-216, 1986.
- 19 Sibulkin, M., *Fire Safety Science-Proceedings of the 1st International Symposium*, 391-400, 1986.
- 20 Wichman, I.S., and Atreya, A., *Combustion and Flame*, 68, 231-247, 1987.
- 21 Hastaoglu, M.A., and Berruti, F., *Fuel*, 68, p. 1408, 1989.
- 22 Alves, S.S., and Figueiredo, J.L., *Chemical Engineering Science*, 44(12), 2861-2869, 1989.
- 23 Di Blasi, C., Crescitelli, S., Russo, G., and Maglione, A., *Proceedings of the First International Conference on Advanced Computational Methods in Heat Transfer*, 209-222, 1990.
- 24 Mikkola, E., *Fire Safety Science-Proceedings of the 3rd International Symposium*, 547-556, 1991.

- 25 Chen, Y., Delichatsios, M.A., and Motevalli, V., *Combust. Sci & Technology*, 88, 309-328, 1993.
- 26 Di Blasi, C., *Combust. Sci & Technology*, 90, 315-340, 1993.
- 27 Di Blasi, C., *Biomass & Bioenergy*, 7, 87-98, 1994.
- 28 Kanury, A.M., *Combust. Sci & Technology*, 97, 469-491, 1994.
- 29 Di Blasi, C., *Ind. Eng. Chem. Res.*, 35, 37-46, 1996.
- 30 Melaaen, M.C., *Numerical Heat Transfer, Part A-Applications*, 29(4), 331-355, 1996.
- 31 Miller, R.S., and Bellan, J., *Combust. Sci & Technology*, 119, 331-373, 1996.
- 32 Yuen, R., Casy, R., De Vahl davis, G., Leonardi, E., Yeoh, G.H., Chandrasekaran, V., and Grubits, S.J., *Proceedings of the 6th Australian Heat & Mass Transfer Conf.*, 257-268, 1996.
- 33 Novozhilov, V., Moghtaderi, B., Fletcher, D.F., and Kent, J.H., *Fire Safety J.*, 25(1), 69-84, 1996.
- 34 Moghtaderi, B, PhD Thesis, The University of Sydney, Australia, 1996.
- 35 Moghtaderi, B., Novozhilov, V., Fletcher, D.F., and Kent, J.H., *Fire & Materials*, 21, 7-16, 1997.
- 36 Moghtaderi, B., Dlugogorski, B.Z., Kennedy, E.M., and Fletcher, D.F., *Fire & Materials*, 22, 155-165, 1998.
- 37 Di Blasi, C., *Int. J. Heat & Mass Transfer*, 41, 4139-4150, 1998.
- 38 Gronli, M.G., and Melaaen, M.C., *Energy & Fuels*, 14, 791-800, 2000.
- 39 Liang, X.H., and Kozinski, J.A., *Fuel*, 79, 1477-1486, 2000.
- 40 Spearpoint, M.J., and Quintiere, J.G., *Combustion and Flame*, 123, 308-324, 2000.
- 41 Di Blasi, C., *Prog. Energy Combust. Sci.*, 19, 71-104, 1993.
- 42 Carslaw, H.S., and Jaeger, J.C., “*Conduction of Heat in Solids*”, 2nd Edition, Oxford University Press, 1959.
- 43 Delichatsios, M.A., and Chen, Y., *Combustion and Flame*, 92, 292-307, 1993.
- 44 Steckler, K.D., Kashiwagi, T., Baum, H.R., and Kanemaru, *Fire Safety Science-Proceedings of the 3rd International Symposium*, 895-904, 1991.
- 45 Antal, M.J., and Varhegyi, G., *Ind. Eng. Chem. Res.*, 34(3), 703-717, 1995.
- 46 Tabatabaie-Raissi, A., Mok, W.S.L., and Antal, M.J., *Ind. Eng. Chem. Res.*, 28, p. 856, 1989.
- 47 Gullet, B.K., and Smith, P., *Combustion and Flame*, 67, p. 143, 1987.
- 48 Barooah, J.N., and Long, V.D., *Fuel*, 55, p. 116, 1976.
- 49 Lewellen, P.C., Peters, W.A., and Howard, J.B., *16th Symp. (Int.) on Combustion*, p. 1471, 1976.

- 50 Wood Handbook, US Forest Products Laboratory, USDA, Agric. Handbook 72, 1987.
- 51 Roberts, A.F., *Combustion and Flame*, 14, 261-272, 1970.
- 52 Lee, C., Chaiken, R.F., and Singer, J.M., *16th Symp. (Int.) on Combustion*, 1976.
- 53 Kanury, A.M., and Blackshear, P.L., *Combust. Sci & Technology*, 2, 5-9, 1970.
- 54 Siau, J.F., "*Transport Processes in Wood*", Springer-Verlag, Berlin, 1984.
- 55 Di Blasi, C., *Chemical Engineering Science*, 53, 353-366, 1998.
- 56 Sahota, M.S., and Pagni, P.J., *International Journal of Heat and Mass Transfer*, 22, 1069, (1979).
- 57 Moghtaderi, B., Novozhilov, V., Fletcher, D.F., and Kent, J.H., *Proceedings of the 1995 Australian Symposium on Combustion and the Fourth Australian Flame Days*, 1995.
- 58 Di Blasi, C., *Fuel*, 75(1), 58-66, 1996.

APPENDIX (A)

Table A1: A summary of selected pyrolysis models of charring solid fuels (Note: Comp. ≡ Comprehensive).

Author	Year	Type	Solution Technique	Kinetic Scheme	Fuel	Description and Main Features
Bamford et al ⁷	1945	Thermal	Analytical	--	Wood	Closed form solution to the heat conduction equation only
Kanury ⁸	1971	Thermal	Analytical	--	Wood	Closed form solution to the heat conduction equation only
Kanury ⁹	1972	Thermal	Numerical (Integral Model)	--	Wood	Approximate solution to the heat conduction equation using a linear temperature profile
Kung ¹⁰	1972	Comp.	Numerical (PDE Model)	One-step global	Wood	One dimensional heat conduction, Convective heat transfer due to volatiles outflow, Variable thermo-physical properties
Kansa ¹¹	1977	Comp.	Numerical (PDE Model)	One-step global	Wood	One dimensional heat conduction, Convective heat transfer due to volatiles outflow, Variable thermo-physical properties, Porous media treatment of the fuel
White et al ¹²	1978	Comp.	Numerical (PDE Model)	One-step global	Wood	One dimensional heat conduction, Convective heat transfer due to volatiles outflow, Variable thermo-physical properties
Tewarson ¹³	1979	Thermal	Algebraic	--	Wood	--
Atreya ¹⁴	1983	Comp.	Numerical (PDE Model)	One-step global	Wood	One dimensional heat conduction, Convective heat transfer due to volatiles outflow, Variable thermo-physical properties, Zero heat of pyrolysis, Moisture desorption model
Delichahtsios et al ¹⁵	1983	Thermal	Analytical	--	Charring fuels	Closed form solution to the heat conduction equation using an integral model approximation

Chan et al ¹⁶	1985	Comp.	Numerical (PDE Model)	One-stage multi-reaction scheme for pyrolysis, One-step global for secondary reactions	Biomass	One dimensional heat conduction, Convective heat transfer due to volatiles outflow, Constant thermo-physical properties, Moisture desorption model
Miller et al ¹⁷	1986	Comp.	Analytical	One-step global	Wood	Closed form solution to the heat conduction equation, Accounts for heterogeneity of the fuel
Parker ¹⁸	1986	Comp.	Numerical (PDE Model)	One-stage multi-reaction scheme	Wood	One dimensional heat conduction, Convective heat transfer due to volatiles outflow, Variable thermo-physical properties, Moisture desorption model, Char shrinkage model
Sibulkin ¹⁹	1986	Comp.	Numerical (PDE Model)	One-step global	Charring materials	One dimensional heat conduction, Internal convective heat transfer
Wichman et al ²⁰	1987	Comp.	Analytical	One-step global	Charring materials	Asymptotic analysis
Hastaoglu et al ²¹	1989	Comp.	Numerical (PDE Model)	Two-stage semi-global reaction scheme	Cellulose	One dimensional heat conduction, Convective heat transfer due to volatiles outflow, Variable thermo-physical properties, Porous media treatment of the fuel, Non-isobaric mass transfer using dusty gas flux equation
Alves et al ²²	1989	Comp.	Numerical (PDE Model)	One-stage multi-reaction scheme	Wood	One dimensional heat conduction, Convective heat transfer due to volatiles outflow, Variable thermo-physical properties, Moisture desorption model
Di Blasi et al ²³	1990	Comp.	Numerical (PDE Model)	Two-stage semi-global reaction scheme	Charring materials	One dimensional heat conduction, Convective heat transfer due to volatiles outflow, Variable thermo-physical properties, Porous media treatment of the fuel, Treats char as a condensed phase

Mikkola ²⁴	1991	Thermal	Analytical	--	Wood	Approximate solution to heat conduction equation, Accounts for the fuel moisture content
Chen et al ²⁵	1993	Thermal	Numerical (Integral model)	--	Charring and non-charring	Approximate solution to the heat conduction equation using an exponential temperature profile
Di Blasi ^{26,27}	1993 1994	Comp.	Numerical (PDE Model)	Two-stage semi-global reaction scheme	Biomass and Wood	One dimensional heat conduction, Convective heat transfer due to volatiles outflow, Variable thermo-physical properties, Porous media, No restriction about tar, In-depth radiation
Kanury ²⁸	1994	Thermal	Analytical	--	Biomass	Closed form solutions to the heat conduction equation under subjected to different boundary conditions
Di Blasi ²⁹	1995	Comp.	Numerical (PDE Model)	Two-stage semi-global scheme	Charring materials	An extension of other Di Blasi's models in which material shrinkage is also taken into account
Melaen ³⁰	1996	Comp.	Numerical (PDE Model)	One-step global	Charring materials	One dimensional, Convective heat transfer due to volatiles outflow, Variable thermo-physical properties, Porous media, Only convective external heat sources
Miller et al ³¹	1996	Comp.	Numerical (PDE Model)	Two-stage semi-global reaction scheme	Cellulose and Wood	One dimensional heat conduction in spherical coordinate system, Convective heat transfer due to volatiles outflow, Variable thermo-physical properties, Porous media treatment
Yuen et al ³²	1996	Comp.	Numerical (PDE Model)	One-step global	Wood	Three-dimensional heat conduction in spherical coordinate system, Convective heat transfer due to volatiles outflow, Variable thermo-physical properties, Porous media
Moghtaderi et al ³³	1996	Comp.	Numerical (PDE Model)	One-stage multi-reaction scheme for pyrolysis	Wood	One dimensional heat conduction, Constant thermo-physical properties, Incorporated into a CFD code for simultaneous solution of solid and gas phases

Moghtaderi ³⁴	1996	Comp.	Numerical (PDE Model)	One-stage multi-reaction scheme for pyrolysis	Wood	One dimensional heat conduction, Convective heat transfer due to volatiles outflow, Variable thermo-physical properties, Moisture desorption model
Moghtaderi et al ³⁵	1997	Thermal	Numerical (Integral model)	--	Charring and non-charring materials	Approximate solution to the heat conduction equation using a quadratic temperature profile
Moghtaderi et al ³⁶	1998	Comp.	Numerical (PDE Model)	One-stage multi-reaction scheme for pyrolysis	Charring materials	One dimensional heat conduction, Convective heat transfer due to volatiles outflow, Variable thermo-physical properties, Moisture desorption model (considers both vapour and liquid phase water), Porous media treatment of the fuel, Accounts for in-depth radiation
Di Blasi ³⁷	1998	Comp.	Numerical (PDE Model)	Two-stage semi-global reaction scheme	Charring materials	An extension of Di Blasi's 1994 model [25] in to a two-dimensional coordinate system, Porous media treatment of the fuel assuming a non-isotropic medium
Gronli et al ³⁸	2000	Comp.	Numerical (PDE Model)	Two-stage semi-global reaction scheme	Wood	One dimensional heat conduction in spherical coordinate system, Internal convective heat transfer, Variable thermo-physical properties, Porous media treatment of the fuel
Liang et al ³⁹	2000	Comp.	Numerical (PDE Model)	One-step global	Biomass	Two-dimensional (cylindrical coordinate), Convective heat transfer due to volatiles outflow, Variable thermo-physical properties, Porous media treatment of the fuel
Spearpoint et al ⁴⁰	2000	Thermal	Numerical (Integral model)	--	Wood	Approximate solution to the heat conduction equation using a quadratic temperature profile